

SDSS J013127.34–032100.1: a candidate blazar with a 11 billion solar mass black hole at $z=5.18$

G. Ghisellini¹, * G. Tagliaferri¹, T. Sbarrato², N. Gehrels³

¹ INAF – Osservatorio Astronomico di Brera, via E. Bianchi 46, I–23807 Merate, Italy

² Univ. di Milano Bicocca, Dip. di Fisica G. Occhialini, Piazza della Scienza 3, I–20126 Milano, Italy

³ NASA–Goddard Space Flight Center, Greenbelt, Maryland 2077, USA

10 March 2021

ABSTRACT

The radio–loud quasar SDSS J013127.34–032100.1 at a redshift $z=5.18$ is one of the most distant radio–loud objects. The radio to optical flux ratio (i.e. the radio–loudness) of the source is large, making it a promising blazar candidate. Its overall spectral energy distribution, completed by the X–ray flux and spectral slope derived through Target of Opportunity *Swift*/XRT observations, is interpreted by a non–thermal jet plus an accretion disc and molecular torus model. We estimate that its black hole mass is $(1.1 \pm 0.2) \times 10^{10} M_{\odot}$ for an accretion efficiency $\eta = 0.08$, scaling roughly linearly with η . Although there is a factor $\gtrsim 2$ of systematic uncertainty, this black hole mass is the largest found at these redshifts. We derive a viewing angle between 3 and 5 degrees. This implies that there must be other (hundreds) sources with the same black hole mass of SDSS J013127.34–032100.1, but whose jets are pointing away from Earth. We discuss the problems posed by the existence of such large black hole masses at such redshifts, especially in jetted quasars. In fact, if they are associated to rapidly spinning black holes, the accretion efficiency is high, implying a slower pace of black hole growth with respect to radio–quiet quasars.

Key words: quasars: general; quasars: supermassive black holes – X–rays: general

1 INTRODUCTION

Yi et al. (2014, hereafter Yi14) discovered SDSS J013127.34–032100.1 (hereafter SDSS 0131–0321) as a radio–loud quasar at a redshift $z = 5.18$ characterised by a large radio to optical flux ratio (i.e. the so–called radio–loudness) $R \sim 100$. Yi14 selected the source through optical–IR selection criteria based on SDSS and WISE photometric data (Wu et al. 2012), and then observed it spectroscopically in the optical and the IR. The IR spectrum revealed an absorbed broad Ly α line and a broad MgII line, that allowed to estimate the black hole mass of the objects through the virial method, yielding $M_{\text{BH}} = (2.7 - 4) \times 10^9 M_{\odot}$. If this were the real black hole mass, then the source would emit above the Eddington limit.

A very large black hole mass found in a jetted quasar at such large redshifts is somewhat puzzling. This is because it is commonly believed that the jet is associated with rapidly spinning black holes, in order to let the Blandford & Znajek (1977) mechanism work. But if this were the case, the efficiency of accretion would be large, implying that *less* mass is required to emit a given luminosity. The black hole would then grow at a slower rate, and it becomes problematic to explain large black hole masses at high redshifts (see e.g. Ghisellini et al. 2013). This motivates our interest in jetted quasars at high redshifts with large black hole masses.

Up to now the three blazars known at $z > 5$ are Q0906+6930 ($z = 5.47$; Romani et al. 2004), B2 1023+25 ($z = 5.3$; Sbarrato et al. 2012, 2013), and SDSS J114657.79+403708.6 ($z = 5.005$; Ghisellini et al. 2014a). All these sources have a well visible accretion disc emission in the IR–optical part of the observed spectral energy distribution (SED), including strong broad emission lines. A large radio–loudness R is a good indicator of the alignment of their jets with the line of sight, that boosts the non–thermal emission because of relativistic beaming. Values $R \geq 100$, as in the case of SDSS 0131–0321 (Yi14), make the source a good *blazar candidate*, i.e. a source whose jet is seen under a viewing angle θ_v smaller than the beaming angle $1/\Gamma$, where Γ is the bulk Lorentz factor of the jet. This definition is somewhat arbitrary, but has the merit to divide in a simple way blazars from their *parent population*, i.e. quasars with jets pointing away from us. The divide at $\theta_v = 1/\Gamma$ implies that for each blazar there are other $2\Gamma^2$ sources of similar intrinsic properties but pointing elsewhere. However, the radio–loudness alone does not guarantee the classification of the source as a blazar: $R > 100$ could in fact correspond to a source seen at $\theta_v > 1/\Gamma$, but with a particularly weak intrinsic optical luminosity, or, vice–versa, with a particular strong intrinsic radio–luminosity. To confirm the blazar nature of these high–redshift powerful sources we require also a strong and hard X–ray flux, because it is an additional signature of a small viewing angle (due to the specific emission mechanism though to produce the X–ray emission, see Dermer 1995 and

* E–mail: gabriele.ghisellini@brera.inaf.it

Sbarrato et al. 2015). For this reason, we asked and obtained a target of opportunity observation in the X-ray band with the *Swift* satellite. In this letter we discuss these data in the broader context of the entire SED, deriving a robust estimate on the black hole mass and on the possible range of viewing angles.

In this work, we adopt a flat cosmology with $H_0 = 70 \text{ km s}^{-1} \text{ Mpc}^{-1}$ and $\Omega_M = 0.3$.

2 SDSS 0131–0321 AS A BLAZAR CANDIDATE

SDSS 0131–0321 was selected by Yi14 as a high- z quasars on the basis of the Sloan Digital Sky Survey (SDSS) and the *Wide-Field Infrared Survey Explorer* (*WISE*) photometric data. The optical and near infrared spectroscopy performed by Yi14 showed a broad Ly α and a MgII line, at $z = 5.18$. From the FIRST (Faint Images of the Radio Sky at Twenty-cm; Becker, White & Helfand, 1995) catalog the radio flux is 33 mJy at 1.4 GHz, corresponding to a νL_ν luminosity of $1.3 \times 10^{44} \text{ erg s}^{-1}$. Yi14 measured a radio loudness of ~ 100 , by assuming that the radio-to-optical spectrum follows a $F_\nu \propto \nu^{-0.5}$ power law, and calculating this way the flux at the rest frame frequencies of 5 GHz and 4400 Å (Kellerman et al. 1989). The source is not detected by the Large Area Telescope (LAT) onboard the *Fermi* satellite. In high- z and powerful radio sources, a radio-loudness equal or larger of 100 strongly suggests that we see the jet radiation with a small viewing angle. This makes SDSS 0131–0321 a good blazar candidate, but in order to confirm it, we need to check if its X-ray emission, produced by the jet, is strong relative to the optical, and if its slope is harder than the one of a typical accretion disc corona (i.e. $\alpha_X < 0.8-1$).

2.1 *Swift* observations

To confirm the blazar nature of SDSS 0131–0321 we asked to observe the source with the *Swift* satellite (Gehrels et al. 2004). In fact the X-ray spectra of blazars beamed towards us are particularly bright and hard, with an energy spectral index $\alpha_x \sim 0.5$ [$F(\nu) \propto \nu^{-\alpha_x}$] (see e.g. Ghisellini et al. 2010, Wu et al. 2013). The observations were performed between October 23 and December 9, 2014 (ObsIDs: 00033480001–00033480014).

Data of the X-ray Telescope (XRT, Burrows et al. 2005) and the UltraViolet Optical Telescope (UVOT, Roming et al. 2005) were downloaded from HEASARC public archive, processed with the specific *Swift* software included in the package HEASOFT v. 6.13 and analysed. The calibration database was updated on June, 2014. We did not consider the data of the Burst Alert Telescope (BAT, Barthelmy et al. 2005), given the weak X-ray flux.

From all the XRT observations we extract a single spectrum with total exposure of 20.2 ks. The mean count rate was $(2.3 \pm 0.3) \times 10^{-3}$. Given the low statistics, the fit with a power law model with Galactic absorption ($N_H = 3.7 \times 10^{20} \text{ cm}^{-2}$, Kalberla et al. 2005) was done by using the likelihood statistic (Cash 1979).

The output parameters of the model were a spectral slope $\Gamma_x = (\alpha_x + 1) = 1.56 \pm 0.38$ and an integrated de-absorbed flux $F_{0.3-10 \text{ keV}} = (1.4 \pm 0.5) \times 10^{-13} \text{ erg cm}^{-2} \text{ s}^{-1}$. The value of the likelihood was 43.9 for 45 dof. The X-ray data displayed in the SED (Fig. 2) have been rebinned to have at least 3σ in each bin.

The source was not expected to be detected in any of the UVOT filters, therefore the various observations were performed with different filters (i.e. the observations were performed with the set-up “filter of the day”), usually W1 or M2 UV-filters. In four cases also the u filter was used, while the b and v filters were used

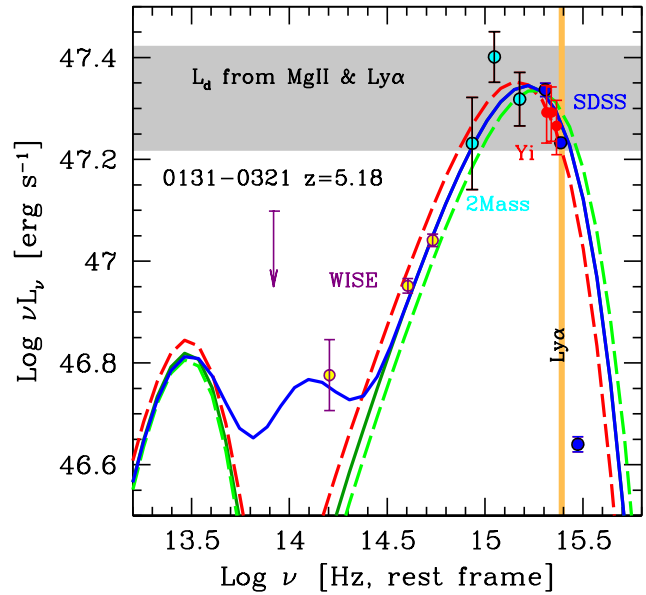


Figure 1. Optical–UV SED of 0131–0321 in the rest frame, together with models of standard accretion disc emission. The grey stripe indicates the νL_ν peak luminosity of the disc, estimated as $L_d = 10 \times L_{\text{BLR}}$ (see text). We show the spectrum of three accretion disc models with different black hole masses: $M_{\text{BH}}/M_\odot = 1.4 \times 10^{10}$ (red dashed), 1.1×10^{10} (solid blue and dark green) and 9×10^9 (dashed, light green). Outside this range of masses, the model cannot fit satisfactorily the data. The *WISE* low frequency point is fitted assuming that, besides the torus emission envisaged by the Ghisellini & Tavecchio (2009) model, there is another, hotter ($T \sim 1300 \text{ K}$) torus component, as found in Calderone et al. (2013).

once during the observation of November 12, 2014 for a total exposures of 223 and 512 s, respectively. The source was never detected. For the v filter we derive a 3σ upper limit of $v \sim 20.5$ mag, corresponding to a flux $F < 0.023 \text{ mJy}$, without accounting for the likely absorption along the line of sight due to intervening matter.

2.2 The accretion disc luminosity

Fig. 1 shows the IR–UV part of the SED, that can be well described as thermal emission from an accretion disc. The peak of this thermal emission lies redward of the hydrogen Ly α frequency (vertical orange line), implying that it is not an artefact of the absorption due to intervening Ly α clouds. This allows to derive the luminosity of the disc rather accurately: $L_d = 4.1 \times 10^{47} \text{ erg s}^{-1}$. The (rest frame) peak frequency of the disc emission is $\nu_{d,\text{peak}} \sim 1.7 \times 10^{15} \text{ Hz}$. Note that L_d is roughly half of the bolometric luminosity L_{bol} estimated by Yi14 on the basis of the (rest frame) 3000 Å continuum luminosity, using the prescription suggested by Richards et al. (2006): $L_{\text{bol}} = 5.18 L(3000 \text{ Å})$. As discussed in Calderone et al. (2013), L_{bol} considered by Richards et al. (2006) includes the IR re-emission by the torus and the X-ray emission, while the “pure” disc luminosity is $L_d \sim 0.5 L_{\text{bol}}$.

The *WISE* low frequency detection point lies in-between the contribution of the accretion disc and the torus emission as modelled by Ghisellini & Tavecchio (2009), who considered that the torus emits as a simple black-body at the temperature of $T_{\text{torus}} = 370 \text{ K}$. In reality, the torus emission is more complex, with emission up to the sublimation dust temperature $T_{\text{subl}} \sim 2000 \text{ K}$ (e.g. Peterson 1997). Calderone et al. (2012) found that composite *WISE* data of a large sample of quasars were consistent with the sum

of two black–bodies with average temperatures $T=308$ and 1440 K and similar luminosities. We have added a black–body with $T = 1300$ K to the model SED, having a luminosity similar to the colder black–body of 370 K. This scenario is probably still oversimplified, but can account for the observed data.

Fig. 1 shows also that the Two Micron All Sky Survey (2MASS, Skrutskie et al. 2006) point at $\log(\nu/\text{Hz}) \sim 15.05$ (rest frame) is above the modelled disc emission. This discrepancy is due to the MgII broad emission line (at 2800 \AA rest frame), falling in the H band filter of 2MASS (Cohen et al. 2003).

The grey stripe in Fig. 1 shows the L_d value inferred from the Ly α and MgII broad lines. We assumed that $L_d \sim 10L_{\text{BLR}}$ (Baldwin & Netzer, 1978; Smith et al., 1981), where L_{BLR} is the luminosity of the entire broad line region, that we derive following the template by Francis et al. (1991): setting to 100 the contribution of the Ly α line, the broad MgII contribution is 34, and the entire L_{BLR} is 555. For the template calculated by Vanden Berk (2001) the contribution of all broad lines to L_{BLR} is similar, with the exception of the Ly α whose contribution is about half the one calculated by Francis et al. (1991).

We then took the logarithmic average of the values derived separately for the MgII and the Ly α line (see data in Yi14), assuming that we see only half of it (i.e. the non absorbed part). We assumed an uncertainty of 0.2 dex on this estimate of L_d .

2.3 The black hole mass

We can set a lower limit to the black hole mass of SDSS 0131–0321 by assuming that its disc emits at or below the Eddington level. This implies $M_{\text{BH}} \geq 3.2 \times 10^9 M_{\odot}$. Yi14, using the virial method (e.g. Wandel 1997; Peterson et al. 2004) applied to the MgII broad line, derived $M_{\text{BH}} = (2.7 - 4.0) \times 10^9$, and concluded that the source is emitting at a super–Eddington rate (they also considered L_{bol} as the disc luminosity).

The IR–optical SED of the source shows a peak and has a low frequency slope consistent with the emission from a simple, Shakura & Sunyaev disc (1973) model. Fig. 2 shows that the non–thermal, possibly highly variable, continuum is not contributing to the IR–UV flux. Since the accretion disc is much less variable than the jet emission, we expect that the IR–UV data, although not simultaneous, give a good description of the disc emission. This depends only on M_{BH} and the mass accretion rate \dot{M} . The latter is traced by the total disc luminosity $L_d = \eta \dot{M} c^2$, where η is the efficiency, that depends on the last stable orbit, hence on the black hole spin (with $\eta = 0.057$ and $\eta = 0.3$ appropriate for a non rotating and a maximally spinning black hole, respectively; Thorne 1974).

Having already measured L_d (hence \dot{M} , assuming $\eta \sim 0.08$), the only free parameter is M_{BH} , whose value determines the peak frequency of the disc emission. For a fixed \dot{M} , a larger M_{BH} implies a larger disc surface, hence a lower maximum temperature. Therefore a larger M_{BH} shifts the peak to lower frequencies. Then the best agreement with the data fixes M_{BH} (e.g. Calderone et al. 2013). Fig. 1 shows the disc emission for three (slightly) different values of M_{BH} : 9, 11 and 14 billions solar masses. Outside this range we do not satisfactorily account for the observed data, while the agreement between the data and the model is rather good within this mass range. We conclude that the black hole mass is well determined and is $M_{\text{BH}} = (1.1 \pm 0.2) \times 10^{10} M_{\odot}$ for $\eta = 0.08$. We obtain $M_{\text{BH}} = 8 \times 10^9 M_{\odot}$ for $\eta = 0.057$ and $M_{\text{BH}} = 2 \times 10^{10} M_{\odot}$ for $\eta = 0.15$ (see also §4). There is thus a factor of $\gtrsim 2$ of systematic uncertainty.

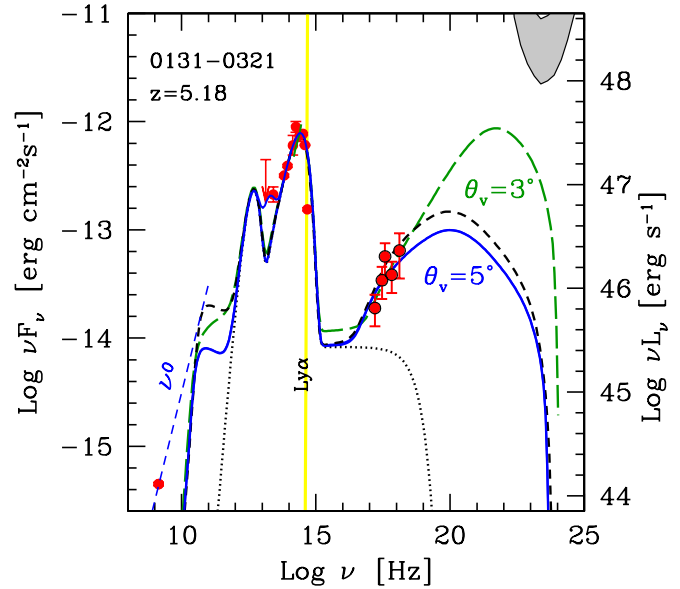


Figure 2. SED of SDSS J0131–0321 together with three one–zone leptonic models, corresponding to $\theta_v = 3^\circ$, $\Gamma = 13$ (green long dashed line); $\theta_v = 5^\circ$, $\Gamma = 13$ (solid blue line) and $\theta_v = 5^\circ$, $\Gamma = 10$ (short dashed black line). Parameters in Tab. 1. The lower bound of the grey stripe correspond to the LAT upper limits for 5 years, 5σ .

3 OVERALL SPECTRAL ENERGY DISTRIBUTION

The overall SED of SDSS 0131–0321 from radio to X–rays is shown in Fig. 2. To guide the eye, the dashed line in the radio domain show a radio spectrum $F_\nu \propto \nu^0$. The 5 years limiting sensitivity of *Fermi*/LAT is shown by the lower boundary of the grey hatched area. The solid and long–dashed lines correspond to the one–zone, leptonic model described in detail in Ghisellini & Tavecchio (2009). The model assumes most of the emission is produced at a distance R_{diss} from the black hole, where photons produced by the BLR and by the torus are the most important seeds for the inverse Compton scattering process, that dominates the high energy luminosity. The region moves with a bulk Lorentz factor Γ and has a tangled magnetic field B . The distribution of the emitting electrons is derived through a continuity equation, assuming continuous injection, radiative cooling, possible pair production and pair emission, and is calculated at a time r/c after the start of the injection, where $r = \psi R_{\text{diss}}$ is the size of the source, and ψ ($=0.1$ rad) is the semi–aperture angle of the jet, assumed conical. The accretion disk component is accounted for, as well the infrared emission reprocessed by a dusty torus and the X–ray emission produced by a hot thermal corona sandwiching the accretion disc.

The three models shown in Fig. 2, whose parameters are listed in Tab. 1, differ mainly from the value of θ_v and Γ . This highlights how the predicted SED changes, especially in the hard X–ray band, by varying θ_v even by a small amount. The two $\theta_v = 5^\circ$ cases indicate the maximum viewing angle that can well explain the existing data. The $\theta_v = 5^\circ$, $\Gamma = 10$ and the $\theta_v = 3^\circ$ cases correspond to a viewing angle smaller than $1/\Gamma$, that would allow to classify SDSS 0131–0321 a blazar. To refine our possible choices we need observations in the hard X–ray band, such as the one that the *Nuclear Spectroscopic Telescope Array* satellite (*NuSTAR*, Harrison et al. 2013) can provide. As in the case of B2 1023+25 (Sbarato et al. 2013), *NuSTAR* could reveal a very hard spectrum, that could make us to choose the large Γ and small θ_v solution. Tab. 1 reports also,

Name	z	R_{diss}	M_{BH}	R_{BLR}	P'_i	L_d	$\frac{L_d}{L_{\text{Edd}}}$	B	Γ	θ_v	γ_b	γ_{max}	P_r	P_B	P_e	P_p
[1]	[2]	[3]	[4]	[5]	[6]	[7]	[8]	[9]	[10]	[11]	[12]	[13]	[14]	[15]	[16]	[17]
0131-0321	5.18	2310	1.1e10	2031	0.02	47.62	0.25	1.6	13	5	70	3e3	46.3	47.2	44.9	47.6
0131-0321	5.18	2310	1.1e10	2031	0.02	47.62	0.25	2.1	10	5	70	3e3	46.0	47.2	44.8	47.4
0131-0321	5.18	2310	1.1e10	2031	9e-3	47.62	0.25	1.1	13	3	300	3e3	46.0	46.9	44.0	46.5
1146+430	5.005	900	5e9	1006	7e-3	47.00	0.15	1.4	13	3	230	3e3	45.9	46.3	44.0	46.5
0906+693	5.47	630	3e9	822	0.02	46.83	0.17	1.8	13	3	100	3e3	46.3	46.2	44.6	47.1
1023+25	5.3	504	2.8e9	920	0.01	46.95	0.25	2.3	13	3	70	4e3	46.0	46.2	44.5	46.9

Table 1. List of parameters adopted for or derived from the model for the SED of 0131-0321, compared with the set of parameters used for the other two blazars at $z > 5$. Col. [1]: name; Col. [2]: redshift; Col. [3]: dissipation radius in units of 10^{15} cm; Col. [4]: black hole mass in solar masses; Col. [5]: size of the BLR in units of 10^{15} cm; Col. [6]: power injected in the blob calculated in the comoving frame, in units of 10^{45} erg s^{-1} ; Col. [7]: logarithm of the accretion disk luminosity (in erg s^{-1}); Col. [8]: L_d in units of L_{Edd} ; Col. [9]: magnetic field in Gauss; Col. [10]: bulk Lorentz factor at R_{diss} ; Col. [11]: viewing angle in degrees; Col. [12] and [13]: break and maximum random Lorentz factors of the injected electrons; Col. [14]–[17]: logarithm of the jet power (in erg s^{-1}) in different forms: Col. [14] power spent by the jet to produce the non-thermal beamed radiation; Col. [15]: jet Poynting flux; Col. [16]: power in bulk motion of emitting electrons; Col. [17]: power in bulk motion of cold protons, assuming one proton per emitting electron. The total X-ray corona luminosity is assumed to be in the range 10–30 per cent of L_d . Its spectral shape is assumed to be always $\propto \nu^{-1} \exp(-h\nu/150 \text{ keV})$.

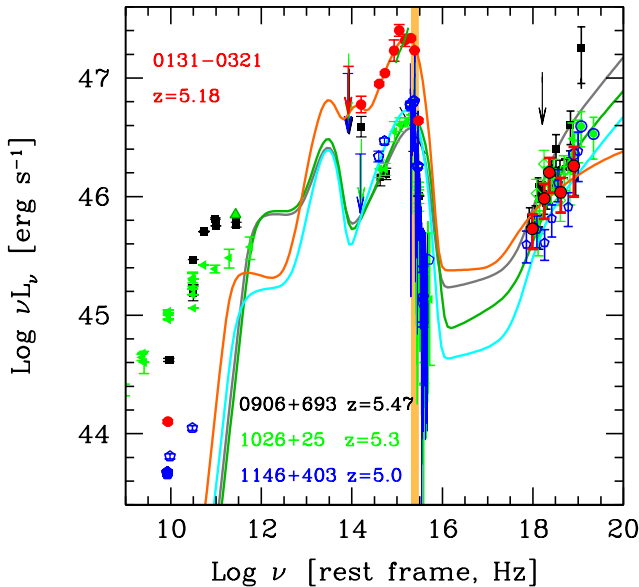


Figure 3. The SED of SDSS 0131-0321 is compared to the SEDs of the other known blazars at $z \geq 5$. SDSS 0131-0321 stands out by having the most powerful disc. The radio and the X-ray data, on the other hand, have luminosity similar to the other blazars. The figure shows also the interpolating models, whose parameters are listed in Tab. 1.

for the ease of the reader, the parameters we used to fit the other 3 known blazars¹ at $z > 5$. The parameters are all very similar, and are also in the bulk of the distribution of parameters accounting for much larger sample of blazars showing broad emission lines (Ghisellini et al. 2010; 2014b, Ghisellini & Tavecchio 2015).

Fig. 3 shows how the SED of SDSS 0131-0321 compares with the SED (in νL_ν vs rest frame ν) of the three other blazar known at $z > 5$. The 4 non-thermal jet SEDs are rather similar, but the accretion disc component of SDSS 0131-0321 stands out, being a factor ~ 4 more luminous.

¹ For the jet powers, we here consider the sum of power of each of the two jets, while in the original papers discussing these sources, the power of only one jet was reported.

4 DISCUSSION AND CONCLUSIONS

Although we cannot decide (yet) if SDSS 0131-0321 can be classified as a blazar in a strict sense (i.e. a source with $\theta_v < 1/\Gamma$), we can nevertheless conclude that θ_v is small, and therefore it is very likely that there exist other sources like SDSS 0131-0321 pointing in other directions. Assuming two oppositely directed jets, $\Gamma = 13$ and $\theta_v = 5^\circ$, we can estimate the presence of other $1/(1 - \cos 5^\circ) = 260$ sources sharing the same intrinsic properties of SDSS 0131-0321 in the same sky area (about 1/4 of the entire sky) covered by the SDSS+FIRST survey. If future *NuSTAR* observations detect a high hard X-ray flux, then the $\Gamma = 13$, $\theta_v = 3^\circ$ solution is preferred, and the total number of sources like SDSS 0131-0321 should be $2\Gamma^2 = 338(\Gamma/13)^2$ in the same sky area.

We believe that the black hole mass we found through the disc-fitting method is very reliable, since we do see the peak of the accretion disc emission red-ward of the Ly α limit. The only uncertainty concerns the use of a simple Shakura and Sunyaev (1973) model, that assumes a no (or a modestly) spinning black hole. On the other hand the resulting fit is good, and we stress that in the case of a fast spinning black hole, with a corresponding high accretion efficiency η , we would derive a *larger* black hole mass. This is because, for a given M_{BH} and \dot{M} , a Kerr black hole would produce more optical-UV flux (with respect to a non spinning black hole), then exceeding the observed data points at the peak of the optical-UV SED. One must lower \dot{M} , but this leads to under-represent the IR-optical point, that can be recovered by increasing the mass (i.e. increasing the disc surface, implying a smaller temperature).

How can such a large mass be produced at $z = 5.18$? At this redshift the Universe is 1.1 Gyr old. Fig. 4 shows the change of the black hole mass in time, assuming different efficiencies η . If the black hole is not spinning, and $\eta < 0.1$, then it is possible to grow a black hole up to 11 billion solar masses starting from a $100M_\odot$ seed if the accretion proceeds at the Eddington rate all the time. But if $\eta = 0.3$, appropriate for a maximally spinning and accreting black hole (Thorne 1974), then the growth is slower, and an Eddington limited accretion cannot produce a $1.1 \times 10^{10} M_\odot$ black hole at $z = 5$, unless the seed is $10^8 M_\odot$ at $z = 20$.

This poses the problem: jetted sources are believed to be associated with fast spinning black holes, therefore with highly efficient accretors. If the accretion is Eddington limited, jetted sources should have black holes *lighter* than radio-quiet quasars with not-

spinning black holes. The solution to this puzzle can be that, when a jet is present, then not all the gravitational energy of the infalling matter is transformed into heat and then radiation, as suggested by Jolley & Kunzic (2008) and Ghisellini et al. (2010). In this case the *total* accretion efficiency can be $\eta = 0.3$, but only a fraction of it (η_d) goes to heat the disc, while the rest ($\eta - \eta_d$) goes to amplify the magnetic field necessary to launch the jet (by tapping the rotational energy of the black hole). The disc luminosity becomes Eddington limited for a greater accretion rate (making the black hole growing faster). This is shown in Fig. 4 as the case $\eta = 0.3$, $\eta_d = 0.1$, that requires a seed of $10^4 M_\odot$ at $z = 20$; and by the case $\eta = 0.3$, $\eta_d = 0.06$, that can reach 11 billion M_\odot starting from a $100 M_\odot$ seed at $z \sim 11$.

In this scenario, the jet *is required* if very large masses must be reached at large redshifts, together with a vast reservoir of mass that can be accreted. In this respect, the recent finding of Punsly (2014), namely that radio–loud objects have a *deficit* of UV emission with respect to radio–quiet quasar of similar disc luminosity, is very intriguing, pointing to the possibility that the inner part of the accretion disc around a Kerr black hole is producing much less luminosity than expected, because the produced energy does not go into heating the disc, but in other forms, such as amplifying the magnetic field of the inner disc, a necessary ingredient to let the Blandford & Znajek process work efficiently.

ACKNOWLEDGEMENTS

This publication makes use of data products from the Wide–field Infrared Survey Explorer, which is a joint project of the University of California, Los Angeles, and the Jet Propulsion Laboratory/Caltech, funded by NASA. It also makes use of data products from the Two Micron All Sky Survey, which is a joint project of the University of Massachusetts and the Infrared Processing and Analysis Center/Caltech, funded by NASA and the National Science Foundation. Part of this work is based on archival data and on–line service provided by the ASI Science Data Center (ASDC).

REFERENCES

Baldwin J.A. & Netzer H., 1978, *ApJ*, 226, 1
 Becker R.H., White R.L. & Helfand D.J., 1995, *ApJ*, 450, 559
 Blandford R.D & Znajek R.L., 1977, *MNRAS*, 179, 433
 Calderone G., Sbarrato T. & Ghisellini G., 2013, *MNRAS*, 431, 210
 Calderone G., Ghisellini G., Colpi M. & Dotti, M., 2013, *MNRAS*, 425, L41
 Cash W., 1979, *ApJ*, 228, 939
 Cohen M., Wheaton Wm.A. & Megeath S.T., 2003, *AJ*, 126, 1090
 Dermer C.D., 1995, *ApJ*, 446, L63
 Francis P.J., Hewett P.C., Foltz C.B., Chaffee F.H., Weymann R.J. & Morris S.L., 1991, *ApJ*, 373, 465
 Gehrels N., Chincarini G., Giommi P. et al., 2004, *ApJ*, 611, 1005
 Ghisellini G. & Tavecchio F., 2009, *MNRAS*, 397, 985
 Ghisellini G., Tavecchio F., Foschini L., Ghirlanda G., Maraschi L. & Celotti A., 2010, *MNRAS*, 402, 497
 Ghisellini G., Haardt F., Della Ceca R., Volonteri M. & Sbarrato T., 2013, *MNRAS*, 428, 1449
 Ghisellini G., Sbarrato T., Tagliaferri G., Foschini L., Tavecchio F., Ghirlanda G., Braito V. & Gehrels N., 2014a, *MNRAS*, 440, L111
 Ghisellini G., Tavecchio F., Maraschi L., Celotti A. & Sbarrato T., 2014b, *Nature*, 515, 376
 Ghisellini G. & Tavecchio F., 2015, *MNRAS*, 448, 1060
 Harrison F.A., Craig W.W., Christensen F.E. et al., 2013, *ApJ*, 770, 103

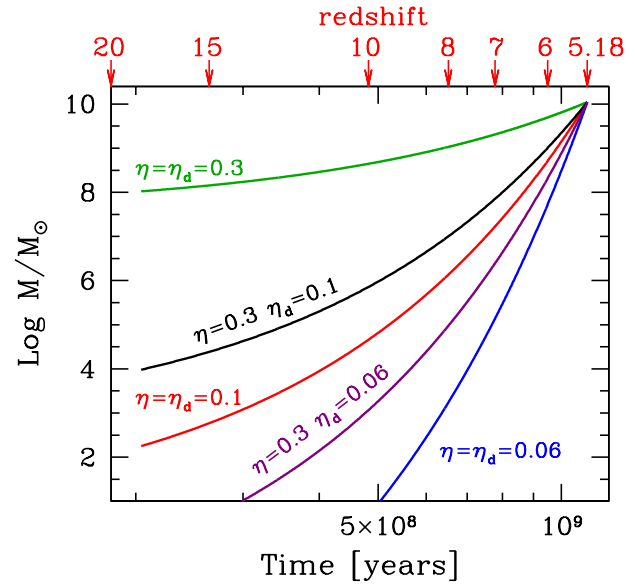


Figure 4. The black hole mass as a function of time in system characterised by an Eddington limited accretion rate, and by different values of the efficiency η (see also Fig. 3 in Trakhtenbrot et al. 2011) Values of $\eta = 0.06$ and $\eta = 0.3$ correspond to no spinning Schwarzschild and maximally spinning Kerr black holes, respectively. All cases corresponds to $M_{\text{BH}} = 1.1 \times 10^{10} M_\odot$ at $z = 5.18$, the mass of SDSS 0131–0321. This figure shows that only if the *accretion disc efficiency* η_d is small we can grow a large mass black hole in the required time starting from a reasonable seed. On the other hand, this may not imply a non rotating black hole.

Jolley E.J.D & Kuncic Z., 2008, *MNRAS*, 386, 989
 Kalberla P.M.W., Burton W.B., Hartmann D., Arnal E.M., Bajaja E., Morras R. & Pöppel W.G., 2005, *A&A*, 440, 775
 Kellermann K.L., Sramek R., Schmidt M. et al., 1989, *AJ*, 98, 1195
 McGreer I.D., Helfand D.J. & White R.L., 2009, *AJ*, 138, 1925
 Peterson B.M., 1997, *An Introduction to Active Galactic Nuclei* Publisher: Cambridge, New York, Cambridge Univ. Press
 Peterson B.M., Ferrarese L., Gilbert K.M. et al., 2004, *ApJ*, 613, 682
 Punsly B., 2014, *ApJ*, 797, L33
 Richards G.T., Lacy M., Storrie–Lombardi L.J. et al., 2006, *ApJS*, 166, 470
 Romani R.W., Sowards–Emmerd D., Greenhill L. & Michelson P., 2004, *ApJ*, 610, L9
 Roming P., Kennedy T., Mason K. et al., 2005, *Space Sci. Rev.* 120, 95
 Sbarrato T., Ghisellini G., Nardini M., et al., 2012, *MNRAS*, 426, L91
 Sbarrato T., Tagliaferri G., Ghisellini G. et al., 2013, *ApJ*, 777, 147
 Sbarrato T., Ghisellini G., Tagliaferri G., Foschini L., Nardini M., Tavecchio F. & Gehrels N., 2015, *MNRAS*, 446, 2483
 Shakura N.I. & Sunjaev R.A., 1973, *A&A*, 24, 337
 Skrutskie M.F., Cutri R.M., Stiening R. et al., 2006, *AJ*, 131, 1163
 Smith M.G., Carswell R.F., Whelan J.A.J et al., 1981, *MNRAS*, 195, 437
 Thorne K.S., 1974, *ApJ*, 191, 507
 Trakhtenbrot B., Netzer H., Lira P. & Shemmer O., 2011, *ApJ*, 730, 7
 Vanden Berk D.E., Richards G.T., Bauer A. et al., 2001, *AJ*, 122, 549
 Volonteri M., Haardt F., Ghisellini G. & Della Ceca R., 2011, *MNRAS*, 416, 216
 Yi W.–M., Wang F., Wu X.–B. et al., 2014, *ApJ*, 795, L29 (Yi14)
 Wandel A., 1997, *ApJ*, 490, L131
 Wu J., Brandt W. N., Miller B.P., Garmire G.P., Schneider D.P. & Vignali C., 2013, *ApJ*, 763, 109
 Wu X.–B., Hao G., Jia Z. et al., 2012, *AJ*, 144, 49